

# Novel High Resolution VGA QWIP detector

H. Kataria\*, C. Asplund, A. Lindberg, S. Smuk, J. Alverbro, D. Evans, S. Sehlin, S. Becanovic,  
P. Tinghag, L. Höglund, F. Sjöström, E. Costard  
IRnova AB, Electrum 236, Kista, Sweden, SE-164 40

## ABSTRACT

Continuing with its legacy of producing high performance infrared detectors, IRnova introduces its high resolution LWIR IDDCA (Integrated Detector Dewar Cooler assembly) based on QWIP (quantum well infrared photodetector) technology. The Focal Plane Array (FPA) has 640×512 pixels, with small (15µm) pixel pitch, and is based on the FLIR-Indigo ISC0403 Readout Integrated Circuit (ROIC). The QWIP epitaxial structures are grown by metal-organic vapor phase epitaxy (MOVPE) at IRnova. Detector stability and response uniformity inherent to III/V based material will be demonstrated in terms of high performing detectors. Results showing low NETD at high frame rate will be presented. This makes it one of the first 15µm pitch QWIP based LWIR IDDCA commercially available on the market. High operability and stability of our other QWIP based products will also be shared.

**Keywords:** QWIP, LWIR, IDDCA

## 1. INTRODUCTION

QWIP technology has established itself as a matured candidate for LWIR photodetector. QWIP based large pixel pitch (30 µm – 25 µm) QVGA and VGA format detectors/IDDCA's are already available on the market. However, no small pitch (15 µm) high resolution QWIP based IDDCA is available on the market, mostly due to the earlier assumption that small pitch QWIP FPAs would not be able to deliver performance at par with other existing technologies. These assumptions have suppressed the real potential of this technology, as cost has for many years been a hurdle when developing and fielding high-end LWIR systems. Smaller linear array based systems are still favored over staring array based systems in some applications purely for cost reasons. In order to address the lack of a cost competitive technology for high-end cooled LWIR detection and adhering to the restraints imposed by the “standardized” 640×512 @ 15 µm pitch format, IRnova has in the last year developed a novel QWIP based VGA detector. Leveraging the advantages of well-established high yielding III-V processing in combination with the inherent stability and robustness of QWIP detectors IRnova is now in a position to offer a technically competitive detector in LWIR at a cost/price point basically on par with the equivalent format in MWIR, finally making the choice between MWIR/LWIR a purely capability driven one.

Earlier works on high resolution QWIP photodetectors have somehow cast an impression that pixel pitch for a LWIR QWIP is limited to ~19 µm. Nevertheless, earlier works by Nedelcu et.al. [1] and their recent work [2] have demonstrated the real potential of QWIP technology even at smaller pixel pitch of 15 µm. This work has successfully demonstrated negligible crosstalk due to photon transfer on unthinned devices. It is understood that with the removal of the substrate further reduction in crosstalk and an increment in the absorption may be achieved.

This article focuses on the development of small pitch (15 µm) QWIP technology for LWIR detection at IRnova using FLIR-Indigo's commercially available ROIC ISC0403. We will first present the results of our performance modelling, based on which FPAs are fabricated and measured. We will present and compare the spectral response of an unprocessed reference wafer and how the response is affected with the subsequent processing. A comparison showing the decrease in absorption of pixels with pitch reduced from 30 to 15 µm can be found in earlier studies done at Thales Research & Technology [3]. Electro-optical performance of test samples consisting of smaller groups of pixels with gratings is used

\* [himanshu.kataria@ir-nova.se](mailto:himanshu.kataria@ir-nova.se); phone +46 72 078 00 38; fax +46 8 519 02 518; [www.ir-nova.se](http://www.ir-nova.se)

to calculate the photoconductive gain, responsivity and dark-current of these devices. Following this, the measurements at FPA level with  $f\#2$  optics, 60 Hz operation will be presented and compared with our initial modelling studies.

## 2. EXPERIMENTAL DETAILS

The QWIP epitaxial wafers were grown on 100 mm GaAs substrates by metal-organic vapor phase epitaxy (MOVPE), as detailed in [4].

Two different techniques were used to characterize the performance of the processed QWIP wafers. The first method makes use of test cells obtained by dicing an array into smaller pieces and flip-chip bonding them with indium bumps to a fan-out chip. After the underfilling and substrate removal process, characterization of the electro-optical performance was made on single pixels, or groups of connected pixels, on the array. This method has the advantage of giving physical access to the pixels for direct measurements of spectral response, dark current and noise without going via a ROIC; see Figure 1.

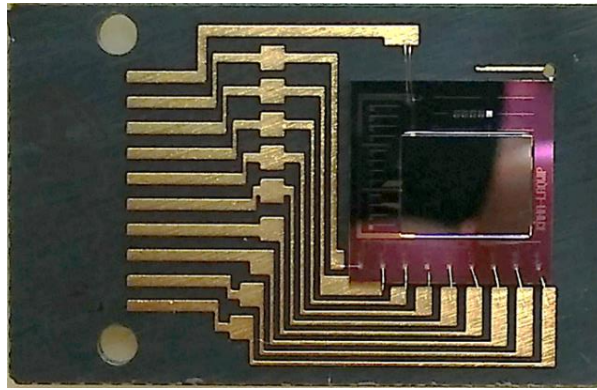


Figure 1. The test cell consists of a part of a thinned-down detector array that is flip-chip hybridized to a silicon fan-out chip. The latter is glued and wire-bonded onto a carrier which mates to the cryogenic electro-optical measurement setup.

The second characterization method consists of image frame recording from a complete FPA in a test setup that is equipped with an appropriate cold shield, as well as the relevant black body targets and is driven by the proxy electronics.

QWIP wafers are processed using IRnova's standard QWIP production line which makes use of sophisticated stepper-based lithography and dry-etching techniques to control the critical parameters like shape and size of the grating dots and pixels, it also allows us to maintain a pixel filling factor higher than 87%. After the completion of the wafer process arrays are diced and cleaned for the hybridization process. For this specific format of arrays ( $640 \times 512 @ 15 \mu\text{m}$  pitch) we have used FLIR-Indigo ISC0403 ROIC for electrically connecting the detectors with the external electronics. Arrays are flip-chip bonded using IRnova's newly acquired state of the art SET FC-300@ die-bonder tool manufactured by SET, France. This new tool and the process developed around it have allowed us to obtain  $\pm 500 \text{ nm}$  post-bonding accuracy. After the flip-chip bonding the hybrids are underfilled with an epoxy to provide mechanical strength to the hybrids during and after the thinning down process (i.e. removal of the GaAs substrate using mechanical and chemical processes). Smaller sized FPAs (referred to as test cells) are also fabricated using the same hybridization process in order to calculate the electro-optical performance of the arrays after the wafer process and hybridization.

After the completion of the thinning down process, the FPAs are mounted on specially designed ceramic carriers with temperature diodes and the FPA performance is measured in a test setup under similar conditions as present in an IDDCA. After an exhaustive set of measurements (see section 3.2) is performed on the FPA it is finally ready to be placed in an IDDCA. Figure 2 shows wafer maps of one of our commercially available QWIP-based gas detectors ( $\text{SF}_6 @ 10.55 \mu\text{m}$  in QVGA format) fabricated using the similar process as described above. This wafer maps demonstrate the maturity of IRnova's III-V MOVPE growth and wafer process technologies in combination with the inherent stability and reproducibility offered by QWIPs.

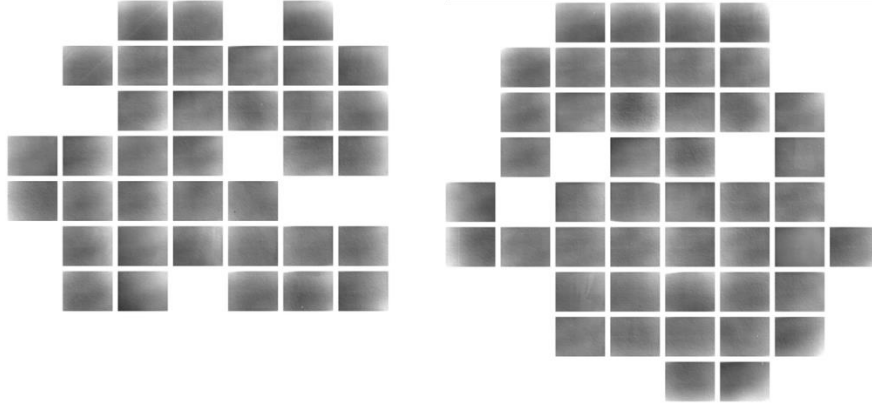


Figure 2. Gain maps (cos4 corrected; grey scale  $\pm 10\%$  of average value) of last 2 wafers from SF<sub>6</sub> production. Few arrays can be seen missing from the wafer map, some arrays are diced for the fabrication of test cells, few are diced to check the process uniformity over the wafer and remaining lost arrays exhibited defects introduced due to particles during the wafer process.

### 3. RESULTS

#### 3.1 Electro-Optical Performance: modelling v/s experiments

Prior to the design and fabrication, the new 15- $\mu\text{m}$  pitch FPA was carefully modeled to predict its performance under realistic operating conditions. For these simulations we used the parameters listed in Table 1 and the measured noise gain shown in Figure 3. The total FPA noise was calculated from the calculated dark and photo currents as

$$n_{tot}^2 = n_{ROIC}^2 + n_{electronics}^2 + n_{dark}^2 + n_{photo}^2,$$

$$\text{where } n_{dark}^2 + n_{photo}^2 = 4eG(I_{dark} + I_{photo})\Delta f \cdot t_{int}^2 = 2eG(I_{dark} + I_{photo})t_{int}.$$

Here,  $G$  is the (dimensionless) noise gain, and  $\Delta f = 1/(2t_{int})$  is the bandwidth corresponding to the frame integration time. The dark and photo currents were obtained as a function of bias and temperature from separate measurements in a test cell (fan-out configuration, no ROIC). As can be seen in Figure 4 the simulation agrees very well with the measured FPA performance without any fitting parameters.

Table 1. Parameters used for simulation of the FPA performance. The ROIC noise and well capacity are the typical values quoted in the ISC0403 manual.

<b>Integration time limit</b>	60 Hz compatible
<b>Detector temperature</b>	70 K
<b>NETD scene temperature</b>	30 °C
<b>Max scene temperature, T_high</b>	70 °C
<b>Well fill @ T_high</b>	95 %
<b>Cold stop aperture F#</b>	2.0
<b>Window transmission</b>	95 %
<b>External electronics noise (rms)</b>	400 e- (4 d.u.)
<b>ROIC noise (rms)</b>	624 e-
<b>ROIC well capacity</b>	6.5 Me-

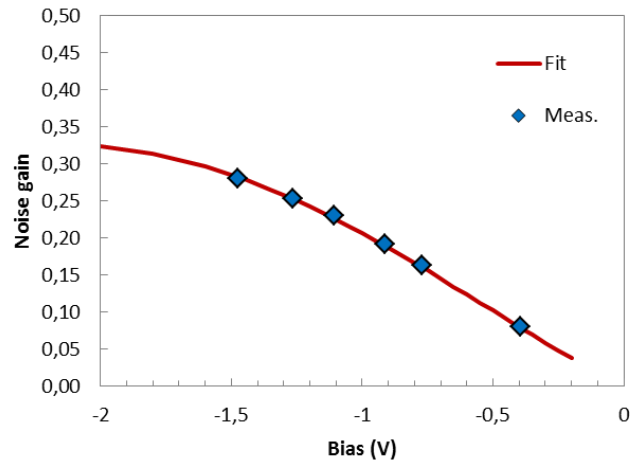


Figure 3. Noise gain of the QWIP structure as obtained on a single-pixel sample under dark conditions at 77 K by dividing the current noise squared by the current:  $G = n_I^2 / 4eI$

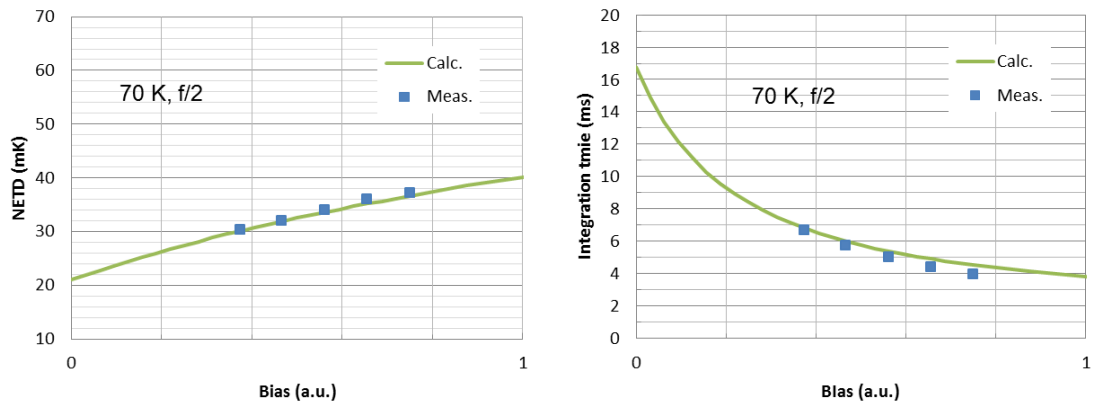


Figure 4. Simulated and measured FPA NETD (left) and integration time (right). A very good agreement is obtained between simulation and measurement without any fitting parameters

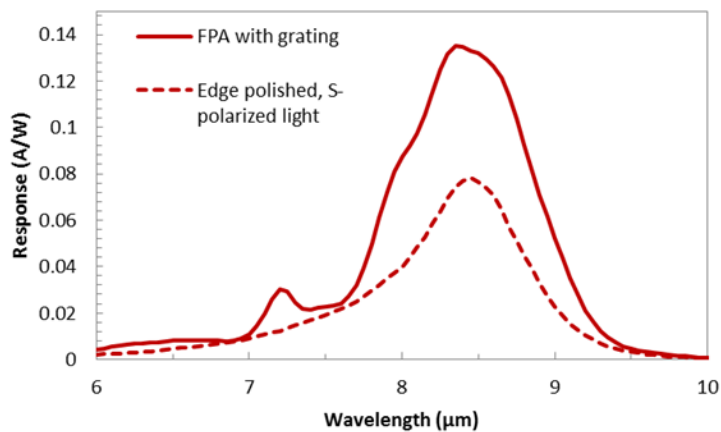


Figure 5. Response spectrum comparison for pixels with and without grating dots, the gratings of the FPA enhances light coupling, resulting in higher response. Peak wavelength is close to 8.5 μm in both cases.

The measured response spectra (70K operating temperature and 1V bias voltage) for a single-pixel QWIP detector without grating and for the fully processed FPA are shown in Figure 5. The grating gives a clear boost to the response, but as expected from the small size of the pixel, the grating efficiency is ~30% lower than for a 25  $\mu\text{m}$  pitch FPA.

### 3.2 FPA performance

FPA performance was evaluated on a fully processed FPA ready for integration into IDCA. The test setup includes a vessel under active pumping integrated with a cooler in the same way as in IDCA. The FPA is temporarily mounted into the setup for characterization. The setup includes also a set of different targets, proxy electronics for driving the ROIC and collecting the data, and software. A cold shield with  $f\#2$  was used for the present evaluation. Integration time was set as the saturation (96 % of well fill) against the blackbody at 70  $^{\circ}\text{C}$ . The targets for the NUC (non-uniformity correction) were at 30 and 50  $^{\circ}\text{C}$ . Temporal NETD was calculated for the target at 30  $^{\circ}\text{C}$  employing 50 collected images. There are many criteria for declaring a pixel non-operable, including exceeding noise, deviating response, continuous output, etc. The limits for the present evaluation were set as strict as for large pixel pitch QVGA format detectors delivered in volumes for high-end applications. Figure 6 show an image of a  $640\times 512$  FPA mounted on a specially designed ceramic carrier, image of the test dewar and the measurement setup.

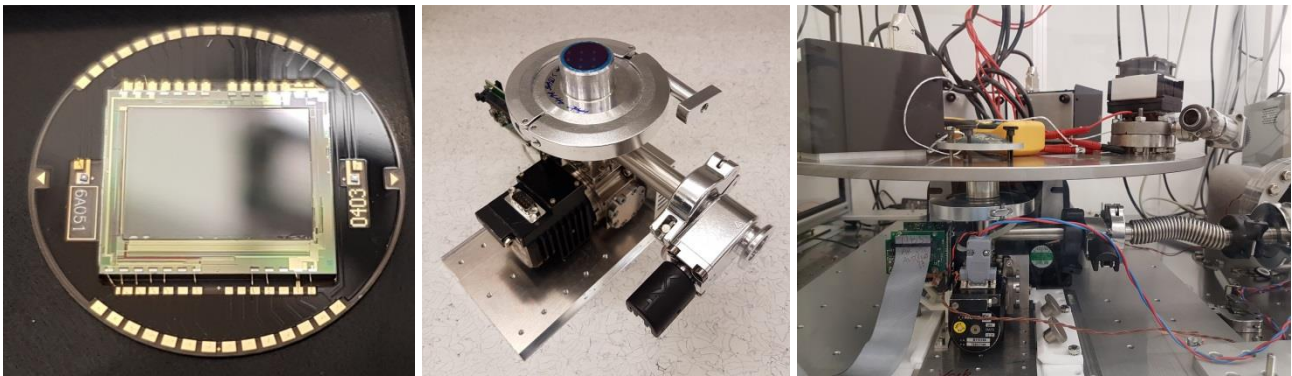


Figure 6. General view of a) an FPA mounted on the ceramic carrier, b) test vessel for FPA characterization, c) station for characterization of FPA.

For the evaluation purposes the measurements were performed at different temperatures and biases. After identifying the optimal bias voltage over the QWIP, another set of measurements was performed for this bias. The results below are presented for the optimized bias. Figure 7 shows experimental data on the temperature dependence of NETD and integration time. The parameters behave exactly as predicted by modelling. Assuming integration time below 7 ms, which is suitable for high frame rate applications, NETD of just above 30 mK was achieved for the projected operation temperature of 70 K. Performance parameters for 70 and 65 K are given in Table 2.

Figure 8 shows NETD histograms for different temperatures, in absolute values (counts vs mK) and normalized by the median value and max number of counts. The distribution is narrow with extremely small number of 50 % outliers, which fall under the NOP criteria. Normalized curves coincide virtually perfect, which is an excellent indication of the stability and predictability of the device. One frame of a video image (Figure 9) shows excellent uniformity and contrast, which is also a sign of negligible crosstalk.

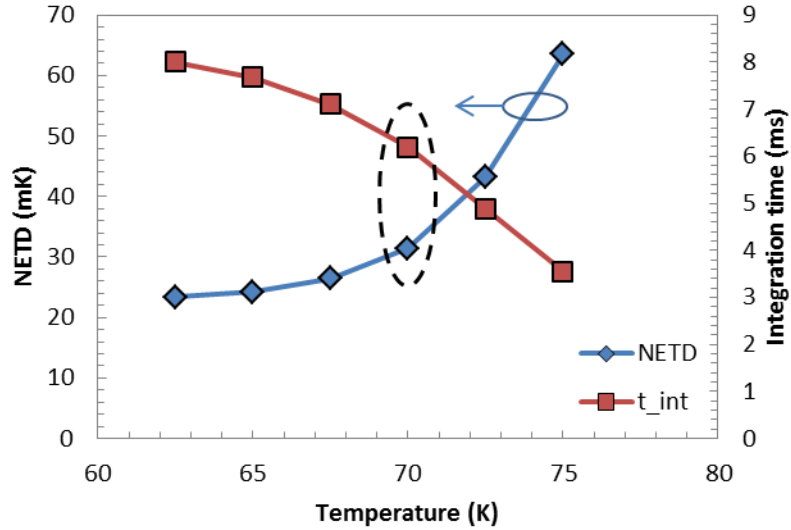


Figure 7. Recorded detector performance with a temperature sweep from 62.5K to 75K

Table 2. Recorded detector performance @ FPA level using optimized bias voltage at different operating temperatures. The integration time is set for 96% well fill at 70°C scene temperature (for very high scene dynamic application). At 70 K operating temperature the NETD is around 30 mK with an integration time suitable for 120 Hz operation.

Detector Performance@ FPA level	Operating @ 65 K	Operating @ 70 K
Integration time (ms)	7.68	6.19
Responsivity (mV/K)	25.3	20.8
Temporal NETD for 30 °C (mK)	24.2	31.5
Spatial NETD for 40 °C (mK)	9.4	13.9

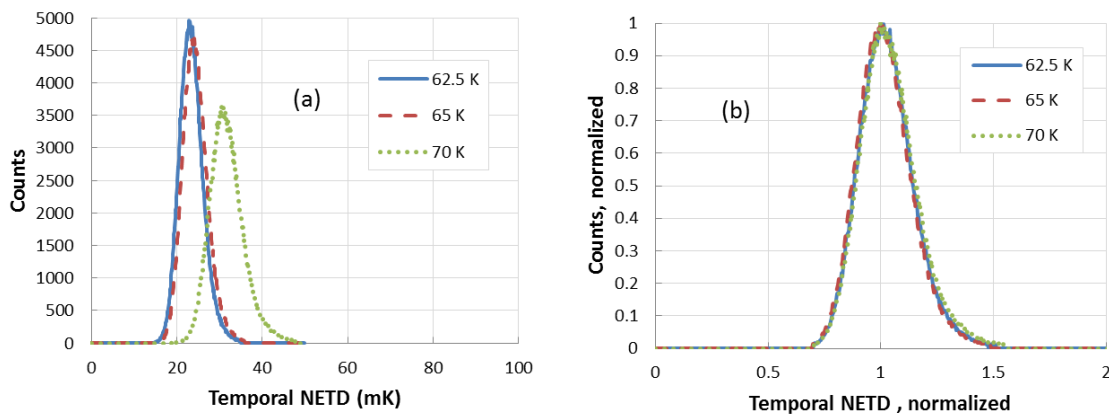


Figure 8. NETD histogram (a) and NETD histogram normalized w.r.t. counts and median value (b) for different FPA temperatures.

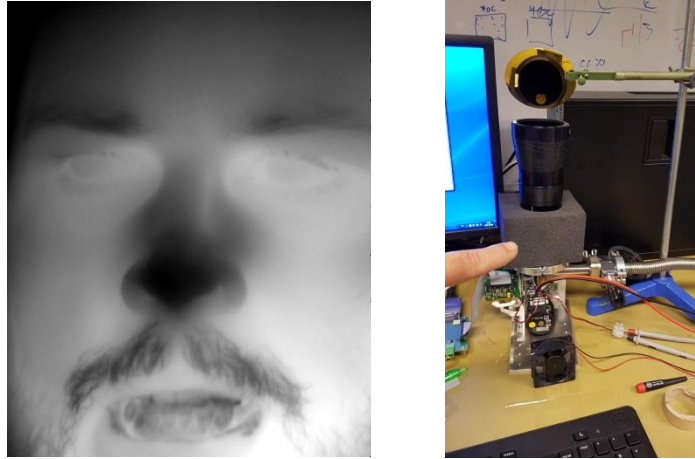


Figure 9. One frame of a video image taken with 640×512 QWIP FPA with @ 15μm pixel pitch. The image is taken with a very basic setup as shown in the adjoining figure

### 3.3 IRnova 640-LW IDDCA: featuring high resolution 640×512 QWIP detector @ 15μm pixel pitch

These high resolution VGA format QWIP arrays are integrated in an IDCA designed for both 640×512 (15 μm pixel pitch) and 320×256 (30 μm pixel pitch) format arrays. It uses the same mechanical and electrical interfaces and supports both QWIP and type-II superlattices technologies. This enables drop-in replacement between IDCA's based on either 320×256 FPAs or 640×512 FPAs and dual-color FPAs. Figure 10 shows an image of the light weight (~550g) IDDCA that delivers LW images with a NETD of <25mK and cool down time of ~6min with a modest power consumption of ~7W (0.5 W cryocooler).



Figure 10. Image of IRnova 640-LW IDDCA

## 4. CONCLUSIONS

This article demonstrates the potential of the QWIP technology even at small pixel pitch (15 μm). By exploiting the stability and uniformity inherent to III-V materials and our state of the art fabrication facilities and capabilities we have demonstrated a highly compact FPA for LWIR detection. First FPAs have exhibited remarkable performance in terms on low NETD (<25mK), short integration times (< 7 ms) and high operability (> 99.9%). This performance matches the demands in place, both for defense and commercial application.

With the launch of a new 640-LW IDDCA, IRnova will redefine the market of LWIR detection. To author's knowledge this is the first commercially available QWIP based IDDCA @ 15 μm pixel pitch.

## 5. ACKNOWLEDGEMENTS

Authors would like to express their gratitude towards the productions group and the optronics group at IRnova for providing processing assistance and for performing a comprehensive set of measurements.

## REFERENCES

- [1] Alexandru Nedelcu, Hugues Facoetti, Eric Costard, Philippe Bois, "Small pitch, large format long-wave infrared QWIP focal plane arrays for polarimetric imagery", Proc. of SPIE Vol. 6542, 65420U, (2007)
- [2] Nedelcu Alexandru, Hamon Gwénaëlle, Dignonnet Adrien, Mathonnière Sylvain, Brière de l'Isle, "Low pitch LWIR QWIPs: Performance level and image quality," Infrared Physics & Technology 70 (2015) 129–133
- [3] E. Costard, Ph. Bois, X. Marcadet, A. Nedelcu, "QWIP and third-generation IR imagers", Proc. SPIE 5978, Sensors, Systems, and Next-Generation Satellites IX, 59781C (2005)
- [4] Henk Martijn, Anders Gamfeldt, Carl Asplund, Sergiy Smuk, Himanshu Kataria, Eric Costard, "QWIPs at IRnova, a status update", Proc. SPIE 9819, 981918 (2016)